Electrical Properties and Defect Chemistry of TiO_2 Single Crystal. III. Equilibration Kinetics and Chemical Diffusion†

M. K. Nowotny, T. Bak, and J. Nowotny*

Centre for Materials Research in Energy Conversion, School of Materials Science and Engineering, University of New South Wales, Sydney, NSW 2052, Australia

Received: January 29, 2006; In Final Form: May 11, 2006

The equilibration kinetics of high-purity single-crystal TiO_2 were monitored using measurements of electrical conductivity in the temperature range 1073−1323 K and oxygen activity, $p(O_2)$, range 10^{-13} to 75 kPa. The kinetics data were used to determine the chemical diffusion coefficient (D_{chem}) within narrow ranges of $p(O_2)$. There was observed a complex effect of the $p(O_2)$ on the D_{chem}, which exhibits a maximum at the n−p transition. The effect of the $p(O_2)$ on the D_{chem} was discussed in terms of the defect disorder and the related semiconducting properties. The activation energy of the D_{chem}, which also varies with the $p(O_2)$, exhibits a maximum at $p(O_2) = \sim 10^4$ Pa (143 kJ/mol).

1. Introduction

Fujishima and Honda[1] were the first to determine that TiO_2 is a good candidate for the photoelectrochemical conversion of solar energy (sunlight) into chemical energy (hydrogen). While this was a major discovery, its commercialization requires a significant increase in the energy conversion efficiency (ECE) from the ∼0.5% reported by Fujishima and Honda[1] to >10%, which the U.S. Department of Energy considers as the benchmark for commercialization.[2] Consequently, many laboratories have undertaken research that aims to process TiO_2 with enhanced properties by modifying its nonstoichiometry, defect disorder, and associated photoelectrochemical properties.

The imposition of controlled defect disorder in metal oxides, such as TiO_2, requires knowledge of the diffusion data and assessment of mass transport kinetics in order to ensure equilibration during processing at elevated temperatures. In particular, these data can be used to determine the required processing conditions, including the time and the temperature of the process. Consequently, a precondition for the fabrication of TiO_2 specimens that are well-defined and reproducible is the determination of diffusion data.

Nonstoichiometry and related defect disorder in nonstoichiometric oxides can be imposed by controlled oxygen activity at the gas−solid interface, which results in the formation of an oxygen chemical potential gradient and the subsequent propagation of the oxygen activity into the bulk. The gradient is the driving force of the equilibration, which is rate-controlled by the transport of defects under the influence of the chemical potential gradient. Consequently, the equilibration aims at annihilation of the concentration gradients. The rate constant of this process, which is the chemical diffusion coefficient (D_{chem}), may be determined from the equilibration kinetics.[3−7]

The determination of well-defined data for the equilibration kinetics requires the following issues to be addressed: (i) The initial and the final stages of the equilibration must be well defined. This is the case when these two stages correspond to gas−solid equilibrium. Therefore, the diffusion data may be considered as well-defined when it is demonstrated that gas−solid equilibrium has been achieved. (ii) When the transport kinetics depend on nonstoichiometry, the D_{chem} must be determined from the equilibration kinetic data within narrow ranges of $p(O_2)$. (iii) The D_{chem} must reflect bulk diffusion under the chemical potential gradient and be independent of surface effects. Therefore, knowledge of the effects of the surface on the gas−solid kinetics is required to assess whether the kinetics are controlled by bulk diffusion or by surface reaction.

The reported data for the D_{chem} of TiO_2 exhibit substantial scatter in both the absolute values and the temperature dependencies.[8−14] The present work demonstrates that, in most cases, the reported data are not well defined because they are reflective of the applied experimental procedures rather than the intrinsic properties of TiO_2. In the remaining cases, the experimental details, which are required to assess physical meaning of the diffusion data, are not available. Therefore, there is a need to determine well-defined data of the chemical diffusion coefficient for TiO_2.

Recently, Lee and Yoo[15] reported so-called 2-fold kinetics, which consists of two independent relaxation kinetics. The related kinetic data are considered in terms of the chemical diffusion coefficients of tetravalent Ti interstitials and oxygen vacancies, which assume comparable values and both are relatively rapid. Their interpretation of data is based on the effect of $p(O_2)$ on electrical conductivity. According to Lee and Yoo,[15] the $p(O_2)$ exponent dependence of the electrical conductivity is −1/5 and −1/6 at low and high $p(O_2)$, respectively. Our electrical conductivity data reported in Part I[16] do not confirm this behavior. The authors of the present work also have reported two regimes of the relaxation kinetics;[17] however, the procedure of the determination of the chemical diffusion coefficient and the interpretation of data differ essentially from those of Lee and Yoo[15] in terms of the assumed defect disorder model. Therefore, the absolute values of their chemical diffusion coefficient cannot be compared with the data determined in the present work.

† This project was performed as part of a UNSW R&D program on solar−hydrogen.

* Corresponding author. E-mail: J.Nowotny@unsw.edu.au. Telephone: 612-9385.6465. Fax: 612-9385.6467.

10.1021/jp060623k CCC: $33.50
Published on Web 08/01/2006

The purpose of the present work is to determine the gas−solid equilibration kinetics for undoped single-crystal TiO_2 within narrow ranges of $p(O_2)$, where the diffusion data are well-defined in terms of the defect disorder.

2. Definition Of Terms

2.1. Defect Disorder. TiO_2 is a nonstoichiometric compound.[3] Its defect disorder has been considered in terms of both oxygen vacancies and titanium interstitials, which result in the formation of donor centers.[3,11] Therefore, TiO_2 has been considered as an n-type semiconductor. Gravimetric studies have revealed that TiO_2 exhibits an effective deficit of oxygen[3]. Therefore, its formula has been assumed as TiO_{2-x}, where x varies between 10^{-2} and 10^{-4}.

It has been shown that TiO_2 may exhibit both n- and p-type properties.[17,18] The presence of p-type properties is considered in terms of titanium vacancies, which are formed during prolonged oxidation of TiO_2.[17] These defects lead to the formation of acceptor centers. Therefore, their imposition in a controlled manner allows the generation of p-type TiO_2 without the incorporation of acceptor-type ions.

Using the Kröger−Vink notation,[19] the following defect equilibria are the most representative for TiO_2:[20]

$$O_O^x \rightleftarrows V_O^{\bullet\bullet} + e' + \frac{1}{2}O_2 \quad (1)$$

$$2O_O + Ti_{Ti} \rightleftarrows Ti_i^{3+} + 3e' + O_2 \quad (2)$$

$$2O_O + Ti_{Ti} \rightleftarrows Ti_i^{4+} + 4e' + O_2 \quad (3)$$

$$O_2 \rightleftarrows V_{Ti}'''' + 4h^{\bullet} + 2O_O^x \quad (4)$$

$$\text{nil} \rightleftarrows e' + h^{\bullet} \quad (5)$$

The relationships between the defect concentrations and the $p(O_2)$ have been derived previously.[16]

Equilibrium constants of the above equilibria were used for derivation of defect concentration diagrams as a function of the $p(O_2)$, which indicate that oxygen vacancies, formed according to eq 1, are the majority defects over a wide range of $p(O_2)$ except under extremely reduced conditions, where the concentration of trivalent titanium interstitials, formed according to eq 2, become the predominant defects.[3,21] It was also shown that the concentration of trivalent Ti interstitials is larger than that of tetravalent Ti interstitials within a wide range of oxygen activities. Moreover, it was shown that Ti vacancies are relatively immobile, and therefore, in the experimental conditions commonly applied in studies of equilibration kinetics, their concentration remains practically constant. Therefore, in the present work, the considerations of the mass transport kinetics during gas−solid equilibration are limited to oxygen vacancies.

Equation 5 represents intrinsic ionization over the band gap. The equilibrium constant of this process was determined elsewhere.[22]

2.2. Electrical Conductivity. Properties such as electrical conductivity may be used to verify the defect disorder models for semiconducting oxides[3]. The physical meaning of the electrical conductivity of TiO_2 at elevated temperatures is complex because ions may have an effect on the conductivity.[20] Previous work by the authors[16] indicates that the transference number of ions (subscript i) in the n−p transition range reaches a substantial value that cannot be ignored. As seen in Figure 1, the ionic transference number for undoped TiO_2 at 1223 K may reach 20%. Consequently, the electrical conductivity of TiO_2 at elevated temperatures should be considered to include three components, related to electrons, holes, and ions:

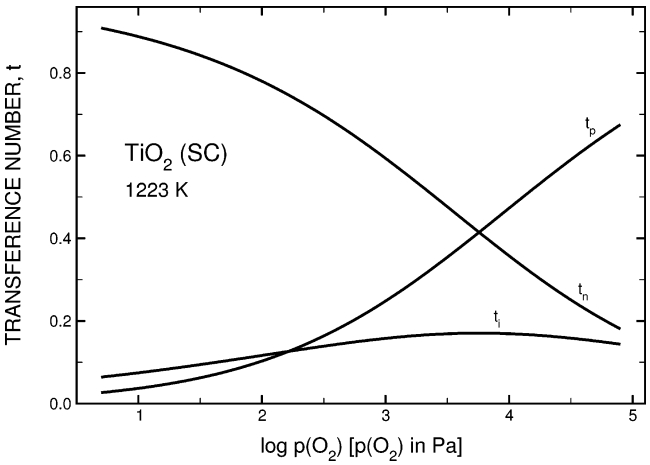

Figure 1. Transference numbers of electronic (t_n, t_p) and ionic (t_i) charge carriers in undoped single-crystal TiO_2 at 1223 K.[16]

$$\sigma = e(n\mu_n + p\mu_p) + z[i]\mu_i = \sigma_n + \sigma_p + \sigma_i \quad (6)$$

where σ is the electrical conductivity, e is the elementary charge, n and p denote the concentrations of quasi-free electrons and electron holes, respectively, μ is the mobility of the charge carrier; and the subscripts n and p refer to electrons and electron holes, respectively, z is the valence of the ionic defect, $[i]$ is the concentration of ions, and the subscript i refers to ions.

2.3. Gas−Solid Kinetics. Defect disorder and the related properties in equilibrium for a oxygen−metal oxide system and the related nonstoichiometry are determined by the $p(O_2)$ in the gas phase and the temperature. Thus, upon equilibration, the concentration of defects is determined by the conditions of equilibrium. When either the $p(O_2)$ or the temperature is changed over an initially equilibrated oxide crystal (within the stability range of a single-phase), the crystal drives toward a new equilibrium state and related nonstoichiometry. The new concentration of defects is imposed at the surface almost immediately and then is propagated into the bulk phase over time, attaining new chemical potentials throughout the crystal. The rate of propagation is determined by chemical diffusion.[4−7] Knowledge of the chemical diffusion rate is essential for the empirical imposition of a uniform concentration of defects within the crystal, free of concentration gradients. Only then is the crystal well-defined and the related properties can be considered to be materials data. Conversely, when the properties are determined under the influence of concentration gradients, then the data are not well-defined and reflect a combination of materials properties and experimental conditions.

The equilibration kinetics is described by the degree of equilibration γ:[23]

$$\gamma = 1 - \prod_{m=1}^{m=3}\left\{\sum_{n=1}^{n=\infty}\frac{2L_m^2\left[\frac{-\beta_n^2 D_{chem}t}{l_m^2}\right]}{\beta_n^2(\beta_n + L_m^2 + L_m)}\right\} \quad (7)$$

where the subscript m refers to the three orthogonal directions of the specimen, L is defined in eq 8, β is the positive root of the equation $L = \beta \tan \beta$, t is the time, l is the half-thickness of the specimen's dimensions, and:

$$L = \frac{l_m k}{D_{\text{chem}}} \tag{8}$$

where k is the rate constant of a nondiffusional surface reaction. In the case where the surface reaction is much faster than bulk diffusion, the equilibration is rate-controlled by bulk diffusion which allows the determination of the D_{chem} from the equilibration kinetics data, as given by Newman:[24]

$$\gamma = 1 - \left(\frac{8}{\pi^2}\right)^3 \left(\sum_{l=0}^{\infty} \frac{1}{(2l+1)^2} \exp\left[\frac{-D_{\text{chem}}(2l+1)^2 \pi^2 t}{a^2}\right] \sum_{l=0}^{\infty} \frac{1}{(2l+1)^2} \exp\left[\frac{-D_{\text{chem}}(2l+1)^2 \pi^2 t}{b^2}\right] \sum_{l=0}^{\infty} \frac{1}{(2l+1)^2} \exp\left[\frac{-D_{\text{chem}}(2l+1)^2 \pi^2 t}{c^2}\right] \right) \tag{9}$$

where a, b, and c are the specimen's dimensions. When oxygen vacancies are the majority defect, which is the case under the present experimental conditions,[17] then γ is defined as:

$$\gamma = \frac{[V_O^{\bullet\bullet}]_t - [V_O^{\bullet\bullet}]_O}{[V_O^{\bullet\bullet}]_\infty - [V_O^{\bullet\bullet}]_O} \tag{10}$$

where the subscripts t, o, and ∞ denote the time, the initial stage of equilibration, and the final stage of equilibration, respectively.

Under conditions of prolonged oxidation of TiO_2, γ assumes a form that is more complex than that expressed by eq 10 because the defect disorder involves an increase in the concentration of titanium vacancies.[17] Therefore, the effects of titanium vacancies on the gas−solid kinetics will be considered subsequently.[25] However, because the present work on the equilibration kinetics does not involve prolonged oxidation, these data are considered in terms of oxygen vacancies.

Assuming that the electrical conductivity is proportional to the concentrations of defects, as described in relation to eq 6, the degree of equilibration may be represented by the following relation:

$$\gamma = \frac{\Delta\sigma_t}{\Delta\sigma_\infty} \tag{11}$$

where $\Delta\sigma_t$ and $\Delta\sigma_\infty$ denote the electrical conductivity change at time t (counted from the moment when the new gas front reaches the surface of the specimen) and at the time at which the new equilibrium state is attained, respectively.

Using Wagner's theory of the oxidation of metals[26,27] and the associated expressions that derive the total ionic particle flux in a growing oxide scale of formula M_aO_b, the following equation may be derived:[28]

$$D_{\text{chem}} = -\frac{k_B T \sigma_i t_{el}}{16 e^2} F^{-1} \tag{12}$$

where k_B is Boltzman's constant, T is the absolute temperature, σ_i is the conductivity component due to ions, t_{el} is the transference number of electronic charge carriers

TABLE 1: Anisotropy for Atomic Diffusion of Cations and Oxygen in TiO_2 According to literature reports[30−35]

authors	ions	temperature [K]	$D_{\parallel c}/D_{\perp c}$
Johnson, 1964[30]	Li^+	773	108
Johnson, 1975[31]	H^+	773	150
Wittke, 1966[32]	Fe^{3+}	Not Stated	$D_{\parallel c} > D_{\perp c}$
Sassaki & Peterson, 1984[33]	Co^{2+}	1073	10^3
Haul & Dumbgen, 1965[34]	O^{2-}	983−1573	$D_{\parallel c} < D_{\perp c}$
Gruenwald & Gordon, 1971[35]	O^{2-}	1079	0.188

[$t_{el} = (\sigma_n + \sigma_p)/\sigma$], and F is:

$$F = \frac{\partial[V_O^{\bullet\bullet}]}{\partial \ln p(O_2)} = -\frac{1}{8}(n+p) \tag{13}$$

The factor F describes the relation between $p(O_2)$ and the change in concentration of the majority defect taking part in the equilibration process. Therefore, the expression for D_{chem}, represented by eq 12, may be rewritten in a form that includes the concentrations of electronic charge carriers:[28]

$$D_{\text{chem}} = \frac{k_B T \sigma_i t_{el}}{2e^2} \frac{1}{n+p} \tag{14}$$

Equation 14 is especially useful in assessing chemical diffusion data within the n−p transition for amphoteric semiconductors, such as TiO_2.

3. Brief Overview of Literature

The crystal structure of rutile, which is the stable high-temperature allotrope of TiO_2, exhibits open channels parallel to the c axis, which is a manifestation of the anisotropy of tetragonal TiO_2[3]. The transport of small cations along these channels is faster than that in the direction perpendicular to the c axis.[29−33] However, oxygen diffusion is faster in the direction perpendicular to the c axis.[34,35] Reported *atomic* diffusion data for cations and oxygen are shown in Table 1. However, the data of Iguchi and Yajima[10] indicate that there is little anisotropy in the transport under chemical potential gradient.

The available data for the D_{chem} of TiO_2, most of which were determined using single crystals, are shown in Figure 2.[8−14] Also, most of these data were determined from the equilibration kinetics monitored using electrical conductivity measurements.

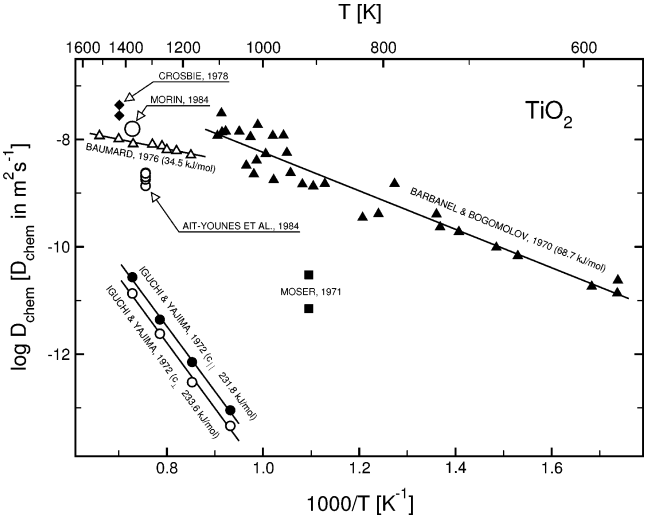

Figure 2. Arrhenius plot of the chemical diffusion coefficient (D_{chem}) for undoped single-crystal and polycrystalline TiO_2 reported in the literature.[8−14]

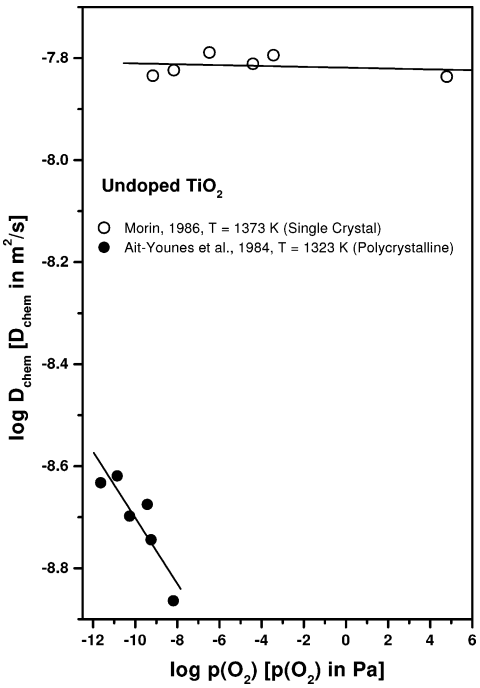

Figure 3. Effect of oxygen activity, $p(O_2)$ on the chemical diffusion coefficient (D_{chem}) for undoped single-crystal and polycrystalline TiO_2 at 1323 K according to Ait-Younes et al.[13] and Morin.[14]

These and other publications generally assume that gas−solid equilibrium is attained when the electrical conductivity reaches a constant value over some length of time, typically 1−2 h. However, this assumption does not take into account the potential for the slope to be only approximately zero and that it might continue to change over an extended time frame. Recent work by the authors on prolonged oxidation of TiO_2[17] demonstrates that the actual slope of the conductivity−time curve becomes measurable only after several hundred hours at elevated temperatures.

As seen in Figure 2, there are substantial discrepancies between the data of the chemical diffusion coefficient reported so far. The reasons for the discrepancy, concerning both absolute values and their temperature dependence, was outlined in the Introduction.

Barbanel and Bogomolov[8] determined D_{chem} data using single-crystal TiO_2 previously outgassed in a vacuum at 973 K. The assessment of their data is problematic because they did not provide details concerning the experimental procedure for the determination of the equilibration kinetics. Especially, their kinetics at 580 K seems to be unrealistic.

The experimental details of the diffusion data of Moser,[9] which were reported by Childs and Wagner,[4] are not available. Therefore, physical meaning of these data is not clear.

Iguchi and Yajima[10] reported D_{chem} data in the range 1073−1373 K. They determined the D_{chem} for the two main crystal orientations. Figure 2 shows that the D_{chem} is slightly larger in the direction parallel to the *c* axis. It was argued that these diffusion data were determined by the transport of oxygen vacancies because (i) they did not observe substantial anisotropy, which would be expected for the transport of cations, and (ii) the activation energies are similar to that determined for oxygen tracer diffusion reported by Haul and Dumbgen.[34]

The study of Baumard[11] reported the equilibration kinetics for single-crystal TiO_2 in the temperature range 1180−1520 K. This study was the first approach to determine the D_{chem} through in situ monitoring of the equilibration kinetics. Baumard claimed that the D_{chem} is independent of the $p(O_2)$.

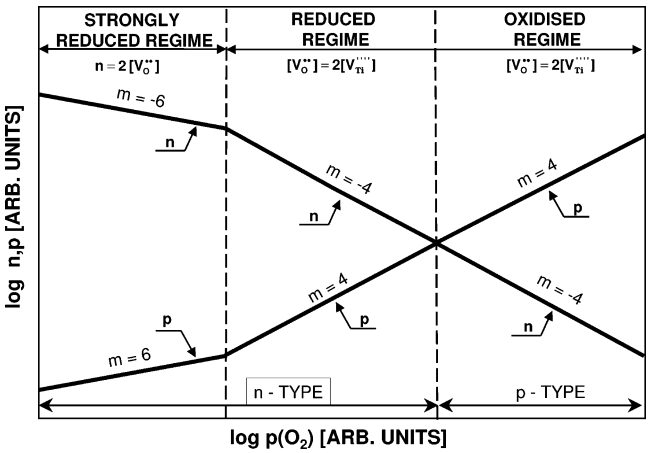

Figure 4. Defect disorder model for undoped TiO_2 showing the effect of $p(O_2)$ on the concentration of electronic charge carriers within ranges of $p(O_2)$ governed by simplified charge neutralities.

Crosbie[12] reported the D_{chem} for polycrystalline TiO_2 with and without dispersed submicron SiO_2 as a function of annealing time. Because no details of the experimental procedure for the determination of the equilibration kinetics were provided, the physical meaning of the reported diffusion data cannot be assessed.

Ait-Younes et al.[13] determined the D_{chem} at 1323 K from the equilibration kinetics determined using the electromotive force of a cell with polycrystalline TiO_2 as an oxygen-sensitive electrode. They reported that the D_{chem} changed as a function of the $p(O_2)$ over the range 10^{-12} to 10^{-8} Pa. Their data are shown in Figure 3, along with those of Morin,[14] who reported that the D_{chem} at the same temperature for single-crystal TiO_2 is effectively independent of the oxygen nonstoichiometry over a large $p(O_2)$ range of 10^{-8} to 10^5 Pa. Assessment of the kinetic data of Morin[14] is not possible because he did not report details of the experimental procedure. It is possible, however, to conclude that the experimental procedures applied by Morin[14] are not well-defined.

The overview of the literature indicates that there is a need to verify the available data for the equilibration kinetics for the O_2−TiO_2 system. The purpose of the present work, and the subsequent work in this series,[25] is to address this need by providing well-defined data for the equilibration kinetics of single-crystal TiO_2. Preliminary kinetics data by the authors indicate that chemical diffusion in TiO_2 is very complex.[36] It also has been shown that the equilibration kinetics of TiO_2 exhibit two kinetics regimes:[17] (i) kinetics regime I (fast kinetics), where the kinetics are determined by the transport of rapid defects; oxygen vacancies; (ii) kinetics regime II (slow kinetics), where the kinetics are determined by the transport of slow defects, i.e., titanium vacancies

The present work aims at the determination of the equilibration kinetics for single-crystal TiO_2 in kinetics regime I and assesses the data of the D_{chem} in terms of the defect disorder, which was derived based on the measurements of both electrical conductivity[16] and thermoelectric power.[37] This defect disorder is shown in Figure 4 in terms of the effect of oxygen activity, $p(O_2)$, on the concentration of electronic defects within the $p(O_2)$ regimes, which correspond to the experimental conditions applied in the present work.

4. Experimental Procedure

Details of the specimen (high-purity single-crystal TiO_2), including its impurity analysis, are reported elsewhere.[16] The

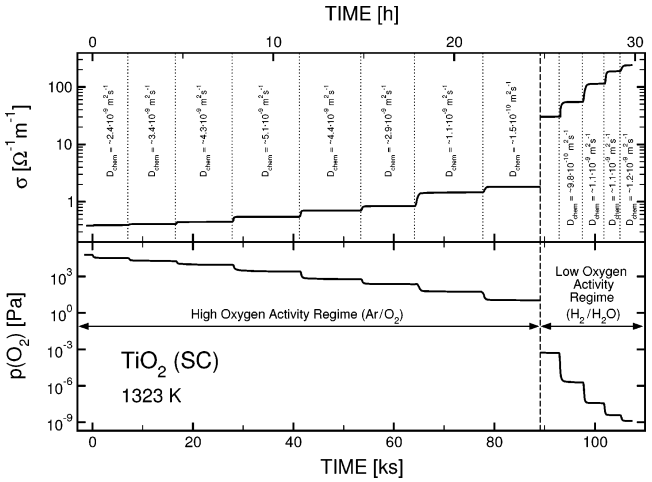

Figure 5. The monitoring sheet for undoped single-crystal TiO_2 at 1323 K showing the changes of oxygen activity during subsequent reduction experiments (lower part) and the related changes of the electrical conductivity within individual experimental cycles at high and low $p(O_2)$.

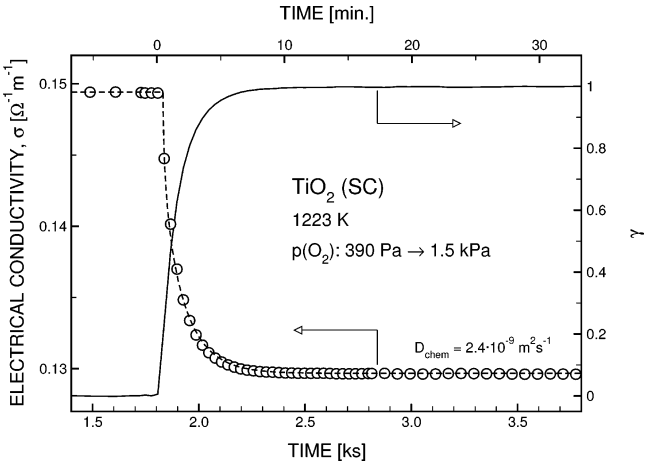

Figure 6. Electrical conductivity (σ) and equilibration degree (γ) as a function of time during oxidation of undoped single-crystal TiO_2 at 1223 K.

size of the specimen was 2 mm × 3 mm × 10 mm; the 3 mm × 10 mm surface was perpendicular to the *c* axis.

The facility for the determination of the electrical conductivity, using the dc four-probe technique, and the experimental monitoring sheet recording the oxygen activity, temperature, and the electrical conductivity, are described in detail elsewhere.[38] The equilibration kinetics were determined in two broad $p(O_2)$ regimes: (i) Low Oxygen Activity Range. The required $p(O_2)$ in this range was imposed by an H_2-H_2O mixtures flowing through the reaction chamber at a constant flow rate of 100 mL/min (set by mass flow controllers). The mixtures were achieved by passing of a mixture of $1\%H_2-99\%Ar$ diluted with pure Ar through deionized water contained in a Drechsel bottle in an ice bath. The $p(O_2)$ levels were imposed in the range $\sim 10^{-13}$ to 10^{-5} Pa within very narrow $p(O_2)$ ranges. (ii) High Oxygen Activity Range. The oxygen activity in this range was imposed by Ar/O_2 mixtures at a constant flow rate of 100 mL/min (set by mass flow controllers) in the range 10 Pa to 75 kPa.

The $p(O_2)$ levels were determined with a zirconia electrochemical oxygen probe. When the $p(O_2)$ was increased or decreased, the experiments are termed *oxidation* and *reduction*, respectively. The equilibration kinetics were determined for both oxidation and reduction runs at six temperatures: 1073, 1198, 1223, 1248, 1273, and 1323 K. The temperatures monitored during the entire equilibration experiment were reproducible to ±0.5 K.

The electrical properties as a function of $p(O_2)$ were assessed using in situ measurements of electrical conductivity and thermoelectic power (*S*).[16,38] These measurements also were used to monitor the equilibration kinetics.

Figure 5 shows a monitoring sheet including the changes of the $p(O_2)$ and electrical conductivity as a function of time within individual cycles of the equilibration during reduction experiments at 1323 K. As seen, the successively reduced $p(O_2)$ in the gas mixture leads to the imposition of appropriately reduced oxygen activity in the reaction chamber in which the specimen is located. The upper part of Figure 5 shows fragments of the related electrical conductivity changes at 1323 K. As seen, the electrical conductivity exhibits changes within 0.5 h. The electrical conductivity was monitored for ~20 h in order to ensure the achievement of equilibrium. In all cases, the electrical conductivity after 2 h reached (within 0.1%) the final electrical conductivity after 20 h.[16,17] Details of the experimental procedure are reported elsewhere.[16]

The condition of the gas−solid equilibrium, corresponding to stable electrical conductivity within 20 h, is referred to as *operational equilibrium*, at which the concentration of oxygen vacancies and also Ti interstials that exhibit comparable diffusion rate, reaches homogeneity. The *operational equilibrium* should be distinguished from the *effective equilibrium*, at which the concentration of Ti vacancies assumes homogeneous distribution. The later term will be discussed elsewhere.[25]

5. Results

The chemical diffusion coefficient was determined using a computer program that allows minimization of the following error function:

$$E_f = \sum (\sigma_{exp} - \sigma_{theor})^2 \qquad (15)$$

where E_f is the error function, σ_{exp} and σ_{theor} denote the experimental data of the electrical conductivity during oxidation−reduction, and σ_{theor} is the theoretical value derived either by the diffusion eqs 7 or 9. In the first attempt, the program adjusted the parameters of eq 7, involving D_{chem}, the rate constant, *k*, and the final conductivity value, σ_∞, in eq 11, to achieve minimum of function E_f. This procedure indicated that the rate constant *k* is ~20 orders of magnitude larger than that of D_{chem}. Therefore, it is concluded that the gas−solid kinetics are determined by bulk diffusion and not surface reaction. Consequently, the D_{chem} was determined assuming that bulk diffusion is the rate controlling the gas−solid equilibration. Then eq 9 was applied. In this attempt, the program iteratively adjusted the parameters of eq 9, involving D_{chem} and the final conductivity value, σ_∞, to achieve minimum of the error function E_f. The stopping criterion was $E_f < 10^{-5}$.

The electrical conductivity data taken for calculations were determined as the average of two conductivity values (current directions of opposite polarity). Figure 6 shows isothermal changes in the electrical conductivity (σ) and the degree of equilibration (γ) during oxidation at 1223 K. As seen, there is an excellent agreement between the kinetics data of $\sigma(t)$ and the kinetic eq 9. The data in Figure 6 are representative for the equilibration kinetic data in the entire range 1073−1323 K.

Figures 7 and 8 show the typical scatter of the data for both reduction and oxidation experiments at high and low $p(O_2)$ ranges at 1248 and 1273 K, respectively. Despite the relatively

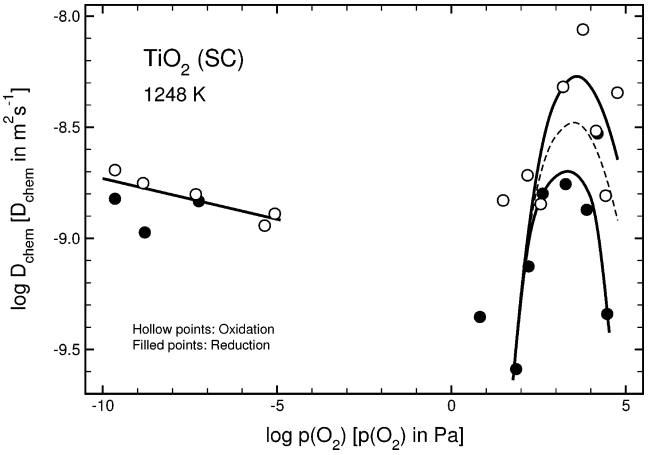

Figure 7. Chemical diffusion coefficient (D_{chem}) for undoped single-crystal TiO_2 at 1248 K as a function of oxygen activity, $p(O_2)$, during oxidation and reduction runs; solid lines in the low $p(O_2)$ range represent the best fit for oxidation and reduction combined; solid lines in the high $p(O_2)$ regime represent the best fit for oxidation and reduction separately; dashed line represents combined values.

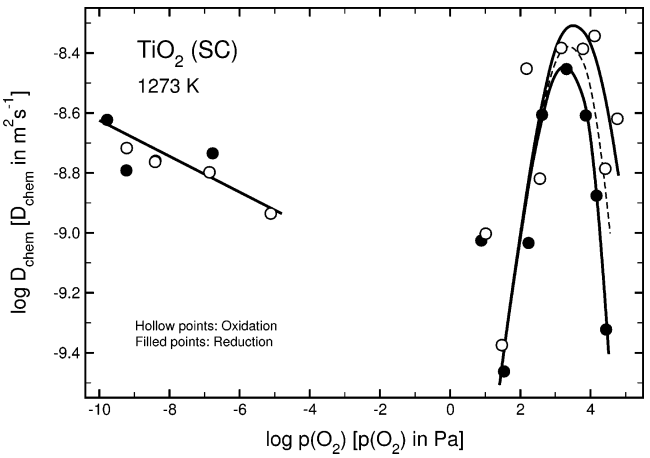

Figure 8. Chemical diffusion coefficient (D_{chem}) for undoped single-crystal TiO_2 as a function of oxygen activity, $p(O_2)$, during oxidation and reduction runs at 1273 K; solid lines in the low $p(O_2)$ range represent the best fit for oxidation and reduction combined; solid lines in the high $p(O_2)$ regime represent the best fit for oxidation and reduction separately; dashed line represents combined values.

large scatter, the reproducibility of the data for successive runs was very good. The scatter of data observed in Figures 7 and 8 is representative for the scatter observed at other temperatures (see Appendix). These data indicate the following: (i) Low $p(O_2)$ Range. The effect of the $p(O_2)$ on the D_{chem} is approximated by a linear dependence for both oxidation and reduction experiments, indicating a weak dependence of the D_{chem} on the $p(O_2)$. The experimental data of the effect of $p(O_2)$ on the D_{chem} for other temperatures (1073, 1198, 1223, and 1323 K) can be seen in the Appendix. (ii) High $p(O_2)$ Range. Despite the substantial scatter of data showing the effect of $p(O_2)$ on D_{chem}, these data allow observation of several behaviors that are apparent at all temperatures: (a) The oxidation kinetics is faster than those for reduction. This can be explained by the segregation-induced diffusion resistance within the electric field of the surface layer.[39] This effect is not apparent at low $p(O_2)$. (b) The effect of the $p(O_2)$ in this range is significant, showing that the D_{chem} increases in the $p(O_2)$ in which n-type conductivity has been identified,[16] assumes a maximum at the n−p transition point, and then sharply decreases. (3) The n−p transition, which

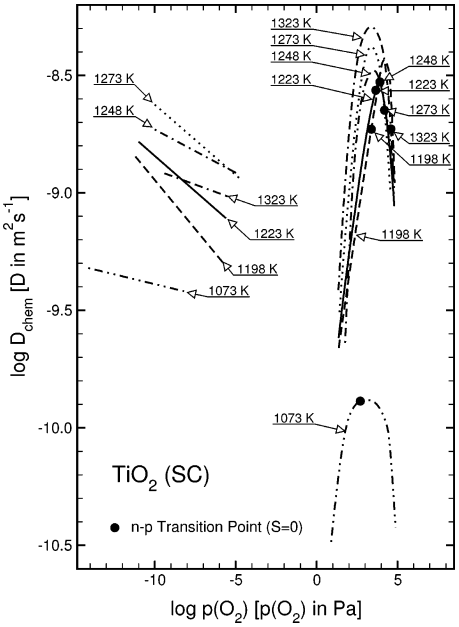

Figure 9. Chemical diffusion coefficient (D_{chem}) as a function of oxygen activity, $p(O_2)$, for undoped single-crystal TiO_2 in the temperature range 1073−1323 K; data points correspond to the n−p transitions determined from the thermoelectric power (S).

was confirmed using measurements of both electrical conductivity and thermoelectric power, coincides with the maximum in the D_{chem}.

The hollow points, representing the data for oxidation, and the filled points, corresponding to reduction, may be approximated by continuous lines, as shown in Figures 7 and 8. In the first approximation, the observed behavior represented by this lines is consistent with the model represented by eq 14. The dashed line, in between these two solid lines, may be used as a general representation of the effect of $p(O_2)$ on the D_{chem} for both oxidation and reduction. This dashed line will then be used for the collective representation of the effect of $p(O_2)$ on the D_{chem} in Figure 9.

Figure 9 shows the effect of the $p(O_2)$ on the D_{chem} over the entire temperature and $p(O_2)$ ranges studied in the present work. For the reason of clarity, Figure 9 includes only the averages D_{chem} for the oxidation and reduction runs and represented by the dashed line in Figures 7 and 8.

The data in Figure 9 indicate the following behavior: (i) The character of the D_{chem} versus $p(O_2)$ dependencies is similar at all temperatures, with the notable exception of the dependence at 1073 K. (ii) The data can be divided into three regimes: (a) strongly reduced (n-type) $10^{-10} < p(O_2) < 10^{-5}$ Pa; (b) reduced (n-type) lower $p(O_2)$ side of the apexes at $\sim 10^3-10^4$ Pa; (c) Oxidized (p-type) higher $p(O_2)$ side of the apexes at $\sim 10^3-10^4$ Pa. The data relevant to the effect of the $p(O_2)$ on the diffusion, including the activation energies, are listed in Table 2. (iii) The n−p transitions determined from the thermoelectric power data[37] are shown as data points. The D_{chem} values appear to reach maxima at the n−p transition points, supporting the consistency of the D_{chem} data with the model described by eq 14. Thus, this indicates that the minima in the concentrations of the electronic charge carriers at the n−p transition points are responsible for the maxima in the D_{chem} values at these points. (iii) The capacity to locate accurately the locations of the apexes is limited owing to the scatter of the data and the steepness of the curves. These are likely to be the causes of the discrepancy between the locations of the apexes and the determined n−p transition points. (iv) The effect of the $p(O_2)$

TABLE 2: Chemical Diffusion Coefficient as a Function of Temperature for TiO_2-SC within Different Defect Disorder Regimes

regime	oxygen activity [Pa]	chemical diffusion coefficient D_{chem} [m^2s^{-1}]
strongly reduced	$p(O_2) < 10^{-5}$	$D_{chem} = 6.21 \times 10^{-6} \exp(-87\ [kJ/mol]/RT)$
reduced	$10 < p(O_2) < p(O_2)_{n=p}$	$D_{chem} = 2.04 \times 10^{-3} \exp(-87\ [kJ/mol]/RT)$
		$D_{chem} = 6.42 \times 10^{-5} \exp(-126\ [kJ/mol]/RT)$
oxidized	$p(O_2) > p(O_2)_{n=p}$	$D_{chem} = 2.22 \times 10^{-6} \exp(-66\ [kJ/mol]/RT)$

on the D_{chem} may be described according to the following generic expression:

$$D_{chem} = (D_{chem})_o\, p(O_2)^{1/n} \tag{16}$$

where $(D_{chem})_o$ is the D_{chem} under standard conditions and $1/n$ is the slope of the dependence of the log D_{chem} versus log $p(O_2)$ plot. The $p(O_2)$ exponent ($1/n$) in the strongly reduced regime is relatively low and varies between $-1/15$ and $-1/40$. These values indicate that the $p(O_2)$ has a very weak effect on the D_{chem} in this range. Conversely, in the reduced and oxidized regimes, the absolute values of the $p(O_2)$ exponents are much greater ($1/n = 1/2$), indicating a significant effect of the $p(O_2)$ on the D_{chem}. These dependencies may be considered in terms of the relevant variables in eq 14, which are electrical conductivity, electronic transference number, and concentrations of electronic charge carriers. (v) The change in the D_{chem} at different temperatures is approximately a half order of magnitude over a wide range of $p(O_2)$ in the strongly reduced regime, while it is over an order of magnitude over narrow ranges of $p(O_2)$ in the reduced and oxidized regimes. (vi) The effect of temperature on the D_{chem} in the strongly reduced regime is consistent, where increasing the temperature increases the D_{chem}. The exception is the data for the highest temperature of 1323 K, which are out of sequence. This effect suggests that the mechanism of chemical diffusion of strongly reduced TiO_2 in this case differs from that of the other temperatures, which may be a result of a change in transport mechanism at temperatures >1273 K.

Figure 10 shows the diffusion data for both single-crystal (reported in this work) and polycrystalline TiO_2 at 1273 K.[40] It can be seen that the D_{chem} values for polycrystalline TiO_2 are smaller than those of single-crystal TiO_2. This difference is likely to be due to grain boundaries acting as weak links for the mass transport during the equilibration. The diffusion in this case is influenced by the grain boundaries, which appear to have a retarding effect on the chemical diffusional transport across grain boundaries.

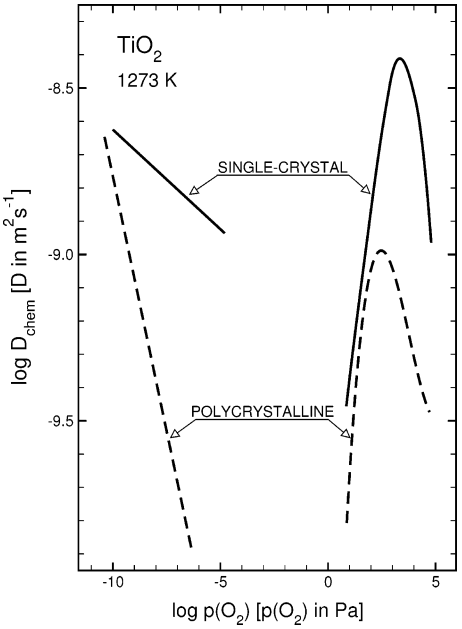

Figure 10. Chemical diffusion coefficient (D_{chem}) for undoped single-crystal and polycrystalline[40] TiO_2 as a function of oxygen activity, $p(O_2)$ at 1273 K.

An error analysis was performed for the data of the chemical diffusion coefficient determined within several independent experiments but for the same specimen studied in identical conditions. For example, at the temperature 1323 K, oxygen activity range, 1.6−6.2 kPa, type of experiment, and oxidation, the analysis resulted in $D_{chem} = (5.4 \pm 0.4)\ 10^{-9}\ m^2\ s^{-1}$ (with the confidence interval 95%).

6. Discussion

6.1. Effect of Oxygen Activity. Figure 9 makes it clear that the effect of the $p(O_2)$ on the D_{chem} is complex. The following general points can be made: (i) The observed character of the D_{chem} versus $p(O_2)$ dependence is unprecedented and is entirely different from those reported for other widely studied semiconducting transition metal oxides such as NiO,[41] CoO,[42,43] and FeO.[43] In all of these cases, however, the D_{chem} data were determined within a regime governed by a single type of charge carrier. Therefore, the main reasons for the observed complex dependence of D_{chem} versus $p(O_2)$ include: large values of nonstoichiometry and the related substantial interactions between defects, and change of the type of the predominant electronic charge carriers within the n−p transition. (ii) The observed nonmonotonic changes in the D_{chem} as a function of the $p(O_2)$ indicate that chemical transport under the influence of a chemical potential gradient exhibits a change in mechanism, which is strongly dependent on the defect disorder, related charge compensation, and concentrations of the predominant charge carriers.

The comments concerning the effects illustrated in Figure 9 prompt the following considerations: (i) TiO_2 is a highly nonstoichiometric compound with several types of ionic defects: oxygen vacancies, titanium interstitials, and titanium vacancies. While the present work does not consider the transport of titanium vacancies because they are immobile under the present experimental conditions, these defects must be considered when evaluating charge neutrality. Also, because titanium interstitials are the minority defects, then they also are ignored. Thus, the diffusion data during equilibration are considered solely in terms of the transport of oxygen vacancies. (ii) An interesting feature in the high $p(O_2)$ range studied is the maxima in the D_{chem} data. The consistency between these maxima and the n−p transition points determined from thermoelectric power measurements indicates that the model described by eq 14 may be applied to explain this effect. (iii) As seen, there is a weak dependence of the D_{chem} on the $p(O_2)$ in a low oxygen activity (strongly reduced) regime. This effect may be interpreted in terms of two factors: (a) The model described by eq 14 indicates that the electrical conductivity, electronic transference number, and concentrations of electronic charge carriers concurrently govern the effect of the $p(O_2)$ on the D_{chem}. (b) Oxygen vacancies in strongly reduced TiO_2 are

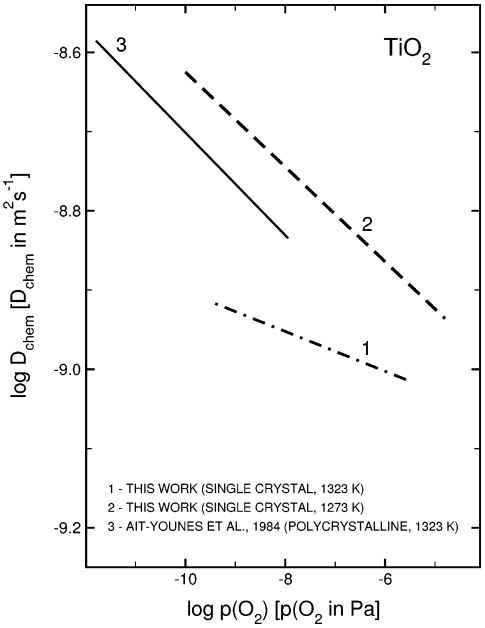

Figure 11. Chemical diffusion coefficient (D_{chem}) as a function of oxygen activity, $p(O_2)$, for undoped single-crystal TiO_2 at 1273 K and 1323 K compared to the data for undoped polycrystalline TiO_2 at 1323 K of Ait-Younes et al.[13]

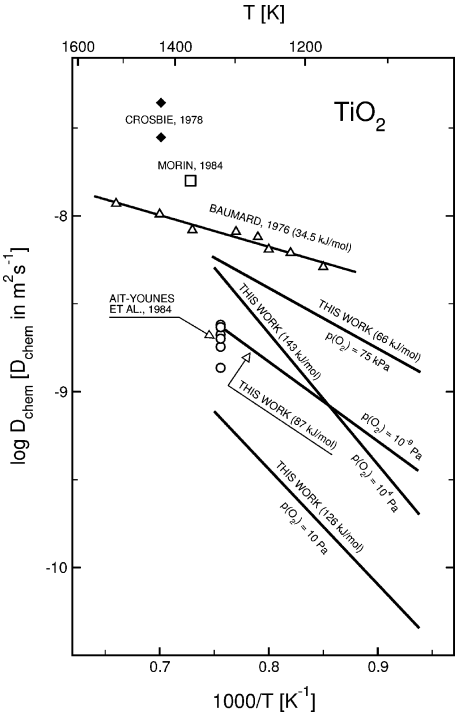

Figure 12. Arrhenius plot of the chemical diffusion coefficient (D_{chem}) for undoped single-crystal TiO_2 along the literature data.

known to form planar defects in the form of shear structures.[3,44] They also are known to interact and form clusters.[45] Consequently, the idealized picture of point defects must be broadened to include larger two- and three-dimensional defect assemblies, which also may have an effect on the dependence of the D_{chem} on the $p(O_2)$.

It is interesting to compare the diffusion data determined in the present work to those elsewhere under comparable experimental conditions. The D_{chem} versus $p(O_2)$ data at 1273 and 1323 K determined in the present work and those reported by Ait-Younes et al.[13] are shown in Figure 11. It can be seen that there

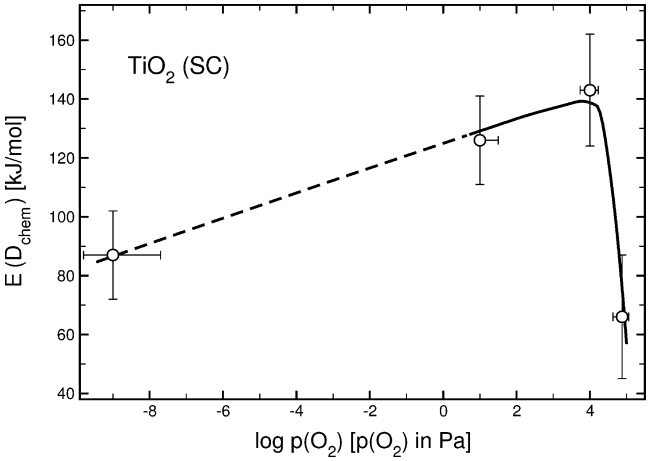

Figure 13. Activation energy of chemical diffusion, $E(D_{chem})$, for undoped single-crystal TiO_2 as a function of oxygen activity, $p(O_2)$, in the temperature range 1073−1323 K.

is clear consistency between the two reports in terms of the effect of $p(O_2)$ on D_{chem} and the proximity of their absolute values.

6.2. Effect of Temperature. Because the D_{chem} varies substantially with the $p(O_2)$, the effect of the temperature on the D_{chem} should be considered within relatively narrow $p(O_2)$ ranges. Figure 12 shows Arrhenius plots of D_{chem} in several ranges of $p(O_2)$, along with those reported by Baumard[11] measured over a wide range of $p(O_2)$ and individual data points reported by Crosbie,[12] Ait-Younes et al.,[13] and Morin.[14] As seen, the absolute values of our data at $p(O_2) = 75$ kPa are slightly smaller than those of Baumard,[11] although our activation energy is twice as large. The consistency between our data and those of Ait-Younes et al.[13] is very good (see Figure 11).

The expressions for the determined D_{chem} as a function of temperature are shown in Table 2 within the specific defect disorder models. The effect of the $p(O_2)$ on the activation energies of the D_{chem}, $E(D_{chem})$, which are shown in Figure 13, confirms that the transport mechanism varies substantially with nonstoichiometry. As seen, the activation energies of the D_{chem} in the reduced regime reach the highest values of 126−143 kJ/mol.

7. Conclusions

The chemical diffusion coefficient of TiO_2 is related closely to the defect disorder. Therefore, D_{chem} should not be considered as a single materials-related datum over the entire range of nonstoichiometry, which is the case for other semiconducting oxides such as NiO.[41]

It has been shown that the gas−solid equilibration kinetic for the O_2−TiO_2 system as well as the D_{chem} exhibit a complex dependence on the $p(O_2)$. Therefore, well-defined data for the D_{chem} of TiO_2 must be determined within narrow ranges of $p(O_2)$ and be considered in terms of its specific nonstoichiometry, defect disorder, and the associated equilibrium $p(O_2)$.

The observed strong effect of the $p(O_2)$ on the D_{chem} within the n−p transition range, involving both the reduction and oxidation regimes, may be explained in terms of minima in the concentrations of electronic charge carriers. In the strongly reduced regime, the effect of the $p(O_2)$ on the D_{chem} for TiO_2 involves the contribution of several concurrent influences, including electrical conductivity, electronic transference number, and concentrations of electronic charge carrier, leading to a weak dependence of D_{chem} on $p(O_2)$.

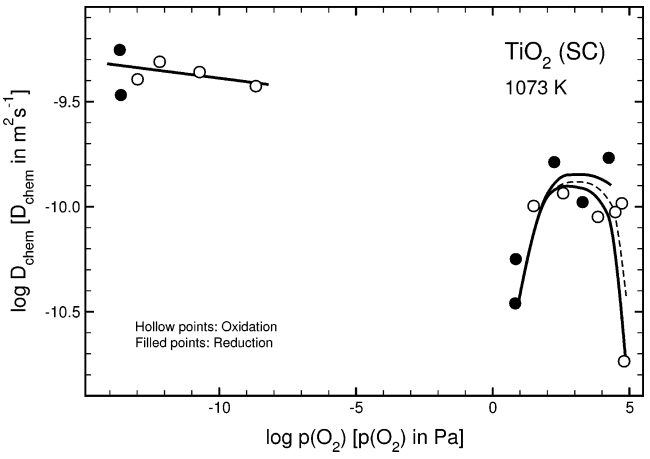

Figure 14. Chemical diffusion coefficient (D_{chem}) for undoped single-crystal TiO_2 at 1073 K as a function of oxygen activity, $p(O_2)$, during oxidation and reduction runs; solid lines in the low $p(O_2)$ range represent the best fit for oxidation and reduction combined; solid lines in the high $p(O_2)$ regime represent the best fit for oxidation and reduction separately; dashed line represents combined values.

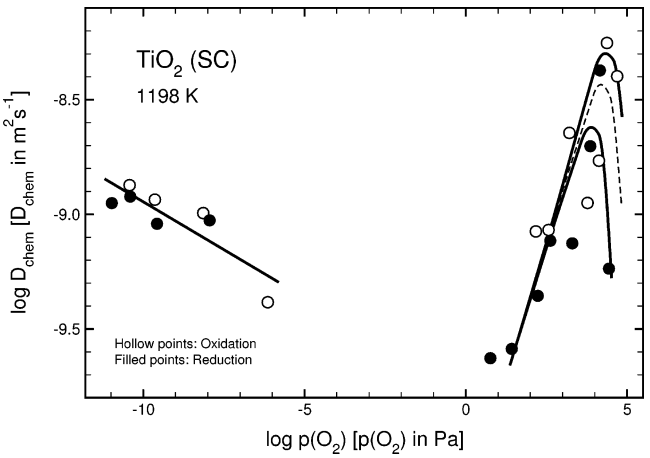

Figure 15. Chemical diffusion coefficient (D_{chem}) for undoped single-crystal TiO_2 at 1198 K as a function of oxygen activity, $p(O_2)$, during oxidation and reduction runs; solid lines in the low $p(O_2)$ range represent the best fit for oxidation and reduction combined; solid lines in the high $p(O_2)$ regime represent the best fit for oxidation and reduction separately; dashed line represents combined values.

The observed effect of $p(O_2)$ on the D_{chem} is consistent with the determined different values of the activation energies for the D_{chem} in different $p(O_2)$ regimes. These sets of data may be used for the selection of optimized processing conditions for TiO_2 under contrtolled $p(O_2)$, including the $p(O_2)$, temperature, and time required to impose a homogeneous nonstoichiometry and the associated concentration of defects within the specimen.

Acknowledgment. The present work was supported by the Australian Research Council, Rio Tinto Ltd., Brickwork Ltd., Mailmasters Pty. Ltd., Sialon Ceramics Pty. Ltd., and Avtronics (Australia), Pty. Ltd.

A. Appendix

The experimental data on the effect of $p(O_2)$ on D_{chem} at 1073, 1198, 1223, and 1323 K are shown in Figures 14−17, respectively.

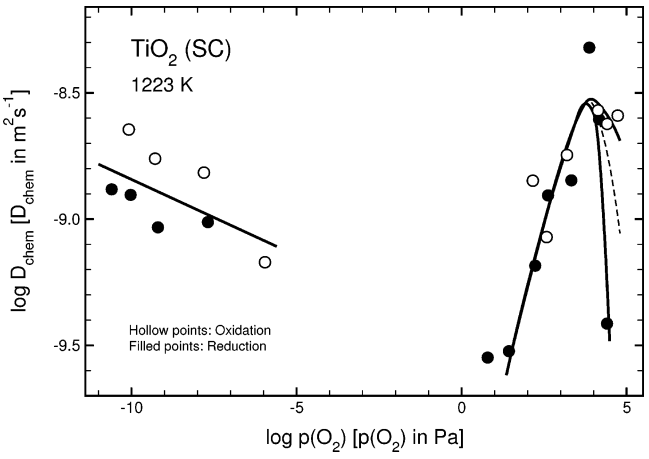

Figure 16. Chemical diffusion coefficient (D_{chem}) for undoped single-crystal TiO_2 at 1223 K as a function of oxygen activity, $p(O_2)$, during oxidation and reduction runs; solid lines in the low $p(O_2)$ range represent the best fit for oxidation and reduction combined; solid lines in the high $p(O_2)$ regime represent the best fit for oxidation and reduction separately; dashed line represents combined values.

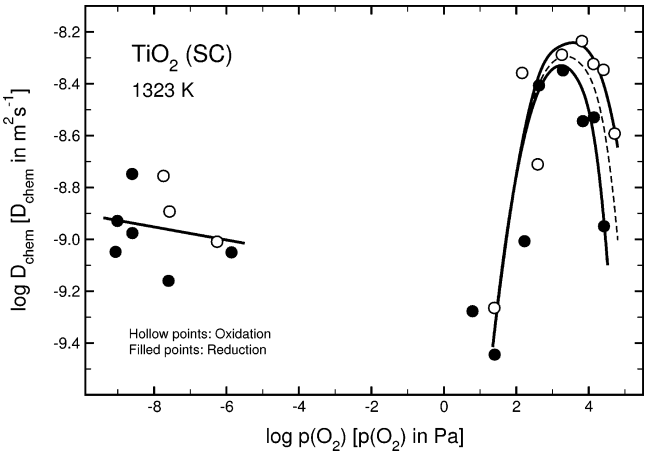

Figure 17. Chemical diffusion coefficient (D_{chem}) for undoped single-crystal TiO_2 at 1323 K as a function of oxygen activity, $p(O_2)$, during oxidation and reduction runs; solid lines in the low $p(O_2)$ range represent the best fit for oxidation and reduction combined; solid lines in the high $p(O_2)$ regime represent the best fit for oxidation and reduction separately; dashed line represents combined values.

References and Notes

(1) Fujishima, A.; Honda, K. *Nature* **1972**, *238*, 378.
(2) Service, R. F. *Science* **2002**, *297*, 2190.
(3) Kofstad, P. *Nonstoichiometry, Diffusion and Electrical Conductivity in Binary Metal Oxides*; Wiley: New York, 1972.
(4) Childs, P. E.; Wagner, J. B., Jr. In: *Heterogeneous Kinetics at Elevated Temperatures*; Bolton, G. R., Worrell, W. L., Eds.; Plenum Press: New York, 1970; p 269.
(5) Levin, R. L.; Wagner, J. B., Jr. *Trans. Met. Soc.* **1965**, *233*, 159.
(6) Price, J. B.; Wagner, J. B., Jr. *Z. Phys. Chem., Neue Folge* **1966**, *49*, 257.
(7) Wagner, J. B. In "Mass Transport in Oxides"; Special Publication 269; National Bureau of Standards: Washington, DC, 1967; p 65.
(8) Barbanel, V. I.; Bogomolov, V. N. *Sov. Phys. Solid State* **1970**, *11*, 2160.
(9) Moser, J. In Childs, P. E.; Wagner, J. B., Jr. *Proc. Brit. Ceram. Trans.* **1971**, *19*, 29.
(10) Iguchi, E.; Yajima, K. *J. Phys. Soc. Jpn.* **1972**, *32*, 1415.
(11) Baumard, F. *Solid State Commun.* **1976**, *20*, 859.
(12) Crosbie, G. M. *J. Solid State Chem.* **1978**, *25*, 367.
(13) Ait-Younes, A.; Millot, F.; Gerdanian, P. *Solid State Ionics* **1984**, *12*, 437.
(14) Morin, F. *Solid State Commun.* **1986**, *58*, 161.
(15) Lee, D.−K.; Yoo, H.-I. *Solid State Ionics* **2006**, *177*, 1.
(16) Nowotny, J.; Bak, T.; Nowotny, M. K. *J. Phys. Chem. B* **2006**, *110*, (Part I, jp0606210), 16270.

(17) Nowotny, M. K.; Bak, T.; Nowotny, J.; Sorrell, C. C. *Phys. Status Solidi* **2005**, *242*, R88.
(18) Bak, T.; Burg, T.; Kang, S.-J. L.; Nowotny, J.; Rekas, M.; Sheppard, L. R.; Sorrell, C. C.; Vance, E. R.; Yoshida, Y.; Yamawaki, M. *J. Phys. Chem. Solids* **2003**, *64*, 1089.
(19) Kröger, F. A.; Vink, H. J. In *Solid State Physics*; Seitz, F., Turnbull, D., Eds.; Academic Press: New York, 1956; p 307.
(20) Nowotny, J.; Sorrell, C. C.; Bak, T.; Sheppard, L. R. In *Materials for Energy Conversion Devices*; Woodhead: Cambridge, U.K., 2005, pp 84−116.
(21) Bak, T.; Nowotny, J.; Rekas, M.; Sorrell, C. C. *J. Phys. Chem. Solids* **2003**, 64, 1057.
(22) Bak, T.; Nowotny, J.; Rekas, M.; Sorrell, C. C. *J. Phys. Chem. Solids* **2003**, *64*, 1043.
(23) Crank, J. *The Mathematics of Diffusion*, 2nd ed.; Oxford University Press: Oxford, U.K., 1975.
(24) Neuman, A. N. *Trans AIChE* **1931**, *27*, 203.
(25) Nowotny, J.; Bak, T.; Nowotny, M. K. *J. Phys. Chem. B* **2006**, (Part IV, jp060624c), 16302.
(26) Wagner, C. *Z. Phys. Chem.* **1933**, *B21*, 25.
(27) Wagner, C. *Prog. Solid State Chem.* **1975**, *10*, 3.
(28) Grzesik, Z.; Bak, T.; Nowotny, J.; Henry, B. *J. Austr. Ceram. Soc*., in press.
(29) Peterson, N. L. *Solid State Ionics* **1984**, *12*, 201.
(30) Johnson, O. W. *Phys. Rev. A: At., Mol., Opt. Phys.* **1964**, *136*, 284.
(31) Johnson, O. W.; Paek, S.-H.; DeFord, J. W. *J. Appl. Phys.* **1975**, *46*, 1026.
(32) Wittke, J. P. *J. Electrochem. Soc.* **1966**, *113*, 193.
(33) Sassaki, J.; Peterson, N. L.; Hoshino, K. *J. Phys. Chem. Solids* **1985**, *46*, 1267.
(34) Haul, R.; Dumbgen, G. *J. Phys. Chem. Solids* **1965**, *26*, 1.
(35) Gruenwald, T. B.; Gordon, G. I *Inorg. Nucl. Chem.* **1971**, *33*, 1151.
(36) Nowotny, M. K.; Bak, T.; Nowotny, M. K.; Sorrell, C. C. *Phys. Status Solidi* **2005**, *242*, R91.
(37) Nowotny, J.; Bak, T.; Nowotny, M. K. *J. Phys. Chem. B* **2006**, *110*, (Part II, jp060622s), 16283.
(38) Nowotny, J. In *The CRC Handbook of Solid-State Electrochemistry*; Gellings, P. J., Bouwmeester, H. J. M., Eds.; CRC Press: Boca Raton, FL, 1997; pp 131−159.
(39) Adamczyk, Z.; Nowotny, J. *J. Phys. Chem. Solids* **1986**, *47*, 11.
(40) Burg, T. Ph.D. Thesis, The University of New South Wales, School of Materials Science and Engineering, in progress.
(41) Nowotny, J.; Sadowski, A. *J. Am. Ceram. Soc.* **1979**, *62*, 24.
(42) Nowotny, J.; Rekas, M. *J. Am. Ceram. Soc.* **1989**, *72*, 1215.
(43) Nowotny, J.; Sadowski, A. In *Transport in Nonstoichiometric Compounds*; Simkovich, G., Eds.; Plenum Press: New York, 1985; pp 227−242.
(44) Matzke, H. J. In *Nonstoichiometric Oxides*; Sorensen, O. T., Academic Press: New York, 1981; pp 156−232.
(45) Stoneham, M. *Phys. Today* **1980**, *33*, 34.